Materials Science Forum Vols. 315-317 (1999) pp. 84-93

Comparison of the Electrochemical- and Gas Phase Hydrogen Sorption Process

A. Züttel[1], D. Chartouni[1], Ch. Nützenadel[1], L. Schlapbach[1], V. Güther[2], A. Otto[2], M. Bärtsch[3] and R. Kötz[3]

[1] University of Fribourg, Physics Institute, Pérolles, CH-1700 Fribourg, Switzerland

[2] Gesellschaft für Elektrometallurgie (GfE), Höfener Strasse 45, DE-90431 Nürnberg, Germany

[3] Paul Scherrer Institute (PSI), CH-5232 Villigen, Switzerland

Keywords: Metalhydrides, Kinetic, Electrodes, AB_5

Abstract

Two families of metal hydrides are mainly used as electrode material for alkaline nickel-metal hydride batteries: the so called AB_5 and the AB_2 intermetallic compounds where A stands for a late transition or a rare earth element and B for one or several early transition elements.

The AB_5 intermetallics crystallize in the hexagonal $CaCu_5$ structure (s.g. P6/mmm, # 191) and form hydrides up to AB_5H_6. A technically widely used AB_5 alloy is $Lm(Ni_{3.6}Mn_{0.4}Al_{0.3}Co_{0.7})$ where Lm stands for La rich mischmetal (≈ 50 wt.% La) M = 422.6 g·mol^{-1}. This alloy is used as electrode material for metal hydride batteries. The reversible capacity at low discharge rates (discharge time > 1 h) is 350 mAh·g^{-1}. Special pretreatments which modify the surface composition of the alloy lead to highly active material. Electrodes of the pretreated alloys can be discharged in less than a 10th of an hour and still deliver more than 200 mAh·g^{-1}.

In this study the hydrogen sorption rate of metal hydrides was investigated in the gas phase and compared to the reaction rate in the electrolyte. In analogy to a pressure step in the gas phase potential steps were applied to the alloy electrodes in an electrochemical half-cell system in order to determine the sorption rates. Comparing the sorption rate in the gas phase with the electrochemical measurements leads to the conclusion that bulk diffusion as well as nucleation and growth of the β-phase cannot be rate determining in the electrochemical charge and discharge reaction, because this part of the reaction is identical for electrochemical and gas phase sorption.

The reaction resistance of the electrodes was directly measured by means of impedance spectroscopy. The sorption rates as well as the resistance are related to the surface composition and surface morphology.

1 Gas phase sorption

The hydrogen gas absorption in pure metals is a process which involves several different but coupled

steps. The steps are coupled in time as well as energetically. The hydrogen absorption in a host metal is energetically best described by the Lennard-Jones potential (Fig. 1) [1]. Molecular diatomic hydrogen gas exists far away from the metal surface. The potential energy of atomic hydrogen is by the dissoziation energy (E_D = 218 kJ·mol^{-1}H, 4.746 eV [1]) higher than molecular hydrogen. If the hydrogen molecule moves close to the metal surface (interface) attractive Van der Waals interactions lead to the formation of the physisorbed state "H_2 + M" ($E_P \approx$ 10 kJ·mol^{-1}H [1]). The following deep minimum describes the chemisorbed state "2H + M" ($E_{ch} \approx$ 50 kJ·mol^{-1}H [1]). The chemisorption requires an activation energy which slows down the kinetics of dissociative absorption and recombinative desorption.

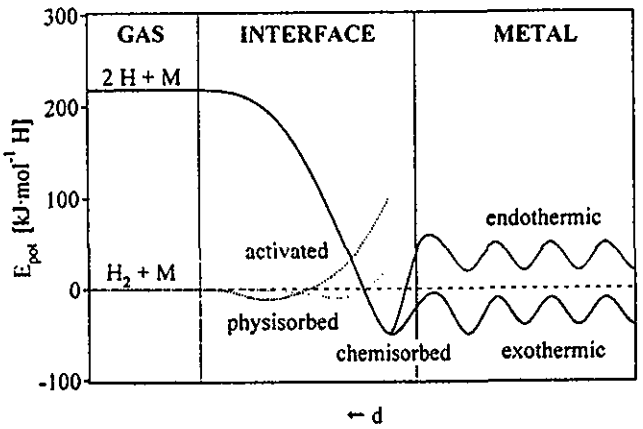

Figure 1: Potential energy E_{pot} for activated and non-activated chemisorption of hydrogen on a clean metal surface and exothermic or endothermic solution in the bulk. A more pronounced minimum just below the surface allows for subsurface hydrogen (one dimensional Lennard-Jones potential [1]). d stands for the distance from the surface

The hydrogen gas absorption on a clean metal surface can be divided into the following steps: 1) physisorption, 2) dissoziation, 3) chemisorption, 4) absorption in the subsurface layer, 5) diffusion within the host metal, 6) nucleation of the hydride phase, and finally 7) growth of the hydride phase. The steps 4 to 7 are identical for gas phase and electrochemical reaction. Each step can be rate determining for the overall reaction of hydrogen with the metal. A review paper on rate equation for a variety mechanism of solid state reactions was published by Sharp et al. [2]. The reaction rate is in general a function of the following parameters: the fraction of material reacted in time, the temperature and the gas pressure. In the beginning of the hydrogen absorption the host metal dissolves some hydrogen as a solid solution (α-phase). As the concentration of hydrogen increases locally the H-H interaction becomes more important and the nucleation and growth of the hydride phase (β-phase) starts. While the two phases (α+β) coexist the equilibrium pressure remains constant because further increase of the hydrogen concentration leads to the growth of the hydride phase. Finally when all the α-phase material is transformed to β-phase some more hydrogen is dissolved in the β-phase and the pressure increases as a function of the hydrogen concentration.

Hydride formation is generally exothermic, the heat evolved is $\Delta Q = T \cdot \Delta S$ with $\Delta S \approx$ 120 J·mol^{-1}·K^{-1} for

hydrogen gas (H_2). The heat evolved leads, at least locally, to a large increase in temperature of the reacting metal. For $LaNi_5$ which reacts to $LaNi_5H_6$ the exothermic reaction heat is approximately 100 $kJ \cdot mol^{-1}$ $LaNi_5H_6$. Considering the heat capacity of $LaNi_5$ (c_p = 136.8 $J \cdot mol^{-1} \cdot K^{-1}$) the temperature increase under adiabatic conditions is in the order of 780 K. The temperature increase is one of the main problems in the investigation of gas phase kinetics of metal hydrides. Goodell et al. [5] have shown that the reaction kinetics for hydrogen absorption and desorption were remarkably improved by increasing the heat transfer in the reactor. This leads to the conclusion, that heat flow is a rate-limiting factor. It was shown [6], that the reaction of $LaNi_5$ with hydrogen gas to $LaNi_5H_6$ (T = 25°C) under optimized heat flow conditions is in less than 2 seconds to 50% completed, and the desorption is in less than 4 seconds to 50% completed. Percheron-Guégan et al. [7] investigated the hydrogen absorption rate of $LaNi_5$ alloy powder in the gas phase. The samples absorbed 80% of their maximum capacity (H/M = 6) in less than 30 seconds. Park et al. [8] found, that the rate-controlling step changes with time from the chemical adsorption of hydrogen molecules on the surface to diffusion of hydrogen through the hydride phase. Finally the reaction is controlled by the growth of the hydride phase. All the above mentioned is valid for uncontaminated surfaces. Flanagan [9] first noticed that reaction rates were markedly inhibited by small pressures of helium. 1 mbar of He reduced the rate of absorption by a factor 3. Goodell et al. [6] observed that the reaction rates depend linearly on the hydrogen gas phase pressure after surface poisoning of $LaNi_5$ with CO, CO_2 and NH_3. This is evidence of a rate-limiting surface steps.

Considering all the above mentioned the rate-limiting mechanism is in general manifold and may also change during the reaction. However, the rate of absorption and desorption can be very high for AB_5 alloys and allows to complete the reaction to 95% in less than a minute.

2 Electrochemical charge- and discharge kinetics

The electrochemical charge and discharge reaction is more complex. The experimental setup of an electrochemical system consists of two electrodes immersed in an electrolyte. Often a third electrode the so called reference electrode is used. The electrodes have to be electrically contacted and the charge state of the electrode is controlled by its electrochemical potential. Similar to the gas phase absorption, the electrochemical charge reaction can be divided into the following steps: 1) physisorption of water molecules, 2) electron transfer and dissoziation, 3) chemisorption, 4) absorption in the subsurface layer, 5) diffusion within the host metal, 6) nucleation of the hydride phase, and finally 7) growth of the hydride phase. The surface of a metal or alloy in the electrolyte also interacts directly with the molecules of the electrolyte. Kuriyama [10] investigated the deterioration behavior of metal hydride electrodes by means of electrochemical impedance spectroscopy. Approximately only one third of the total resistance in the measurement is due to the reaction resistance. Two thirds were due to the electrodes morphology dependent resistance's. The reaction resistance and the resistance of the electrolyte are strongly temperature dependent. A decrease of 10°C in temperature doubles the reaction resistance and the conductivity of the electrolyte decreases by approximately 30%.

Züttel et al. [11] investigated the influence of the electrode thickness on the overpotential during charge and discharge using a $MmNi_{3.6}Mn_{0.3}Al_{0.4}Co_{0.7}$ (Lm: 52% La, 33% Ce, 11% Nd, 3% Pr) alloy. The absolute value of the overpotentials are equal for charge and discharge. The charge/discharge kinetics are expected to depend on the reaction mechanism and on the electrode morphology. The analysis of a series of electrodes with different thickness has demonstrated, that the total electrode resistance increases linearly with the thickness (d) of the electrode $R = 0.12\ \Omega{\cdot}g + 1.91\ \Omega{\cdot}g{\cdot}mm^{-1}{\cdot}d\cdot A^{-1}{\cdot}\rho^{-1}$ where (A) stands for the geometrical electrode surface and (r) for the density of the compacted electrode material. Fukumoto [12] investigated the effect of the stoichiometric ratio on the electrochemical properties of negative electrodes for the alloys with the composition $Mm(Ni_{3.6}Mn_{0.4}Al_{0.3}Co_{0.7})_a$ (Mm: 52.6% Ce, 24.9% La, 5.6% Pr, 16.9% Nd and 0.14% Sm) and $0.88 \le \alpha \le 1.12$. The unit cell volume as well as the discharge capacity (i_{dis} = 200 $mA{\cdot}g^{-1}$) of the alloys decreases in the range of $0.96 \le \alpha \le 1.12$. In the same range of α the plateau pressure increases, i.e. the stability of the hydrides decreases. The exchange current density depends linearly on the plateau pressure (p_{eq}) $i = 415\ mA{\cdot}g^{-1} + 100\ mA{\cdot}g^{-1}{\cdot}bar^{-1}{\cdot}p_{eq}$.

Iwakura et al. [13] determined the activation energy (E_a) for hydrogen absorption of the electrodes from the peak current in the polarization curve. The activation energy of a series of $Mm(Ni_{3.6}Mn_{0.4}Al_{0.3}Co_{0.7})\alpha$ alloys with $0.88 \le \alpha \le 1.12$ depends on α according to the following equation

$$E_a\ [kJ{\cdot}mol^{-1}] = 10.4 + 72.6{\cdot}\alpha - 56.3{\cdot}\alpha^2 \quad (1)$$

Furthermore, it was shown that the discharge efficiency correlates linearly with the activation energy as well as with the exchange current density.

During the discharge process, either hydrogen diffusion in the bulk of the alloy or the charge transfer at the surface of the negative electrode should be the rate determining step [14]. Since the alloy with the composition α = 0.88 forms a more stable hydride, it is supposed that the rate of hydrogen diffusion is relatively slow, resulting in a smaller discharge capacity.

In contrast to the gas phase reaction, where the interface is gas-solid and the rate of diffusion of the hydrogen in the gas phase is very high, the electrochemical charge and discharge reaction occurs at the liquid-solid interface. At room temperature and atmospheric pressure the hydrogen concentration in the gas phase is approximately 0.05 $mol{\cdot}l^{-1}$ and the average molecular speed for hydrogen is 622 $m{\cdot}s^{-1}$. In the electrolyte the water concentration is 55 $mol{\cdot}l^{-1}$ and the average speed of an ion is in the order of $5{\cdot}10^{-4}$ $m{\cdot}s^{-1}$ (electrodes 0.1 mm apart and a potential of 1 V). This simple comparison leads to the conclusion that the diffusion of the reacting molecules to the metal surface is in the gas phase 10^3 times faster compared to the electrolyte.

In this paper the rate of gas phase absorption and desorption is compared with the rates found for the electrochemical charge and discharge reaction.

3 Experimental

3.1 Alloy preparation:

Three alloys with the composition $Lm(Ni_{3.6}Mn_{0.4}Al_{0.3}Co_{0.7})\alpha$ (Lm: 50% La, 35% Ce, 3.5% Pr, and 11% Nd) and α = 0.96, 1.02 and 1.1 ($AB_{4.82}$, $AB_{5.08}$ and $AB_{5.48}$) were melted in a vacuum induction furnace.

3.2 Electrochemical tests:

For the electrochemical measurements approximately 25 mg of the alloy powder was mixed with copper powder (Merck p.a. < 63 μm) in the weight ratio of 1:3 and cold pressed (p = 500 MPa) to a pellet (d = 7 mm). The pellets were fixed on a nickel holder with a cylindrical PTFE-clip. The electrodes were charged and discharged electrochemically in a 6 M KOH electrolyte in an open standard electrochemical cell. A nickel plate was used as counter electrode and potentials were referred to a Hg/HgO reference electrode [15]. The discharge cut-off potential was set to -0.6 V vs.. Hg/HgO reference electrode. The electrodes were cycled with constant charge and discharge current (300 $mA \cdot g^{-1}$).

3.3 Potential step:

In order to compare constant pressure gas phase absorption and desorption measurements with electrochemical measurements the electrodes were set to a constant potential and the current was measured. The current represents the rate of absorption or desorption and the integrated current corresponds to the change in hydrogen content.

3.4 Equilibrium potential measurements:

The equilibrium potentials were measured in a pulsed cycle, i.e. the current was applied for a short time (8 minutes) and after a pause of 3 minutes the potential was measured. This procedure was repeated 50 times until the electrode was completely charged. After that the equilibrium potential of the discharge branch were determined the same way.

3.5 Electrode resistance:

The overpotential, i.e. the potential of the electrode with applied current minus the equilibrium potential was measured as a function of current and temperature. A current pulse, i.e. a constant current for three minutes, was applied and the potential was measured. Thereafter the electrode was put on open circuit and the equilibrium potential was measured after a pause of three minutes. This procedure was repeated with increasing charge and discharge currents (Tafel plot). The slope of the line od overpotential versus current is proportional to the specific resistance of the electrode.

3.6 Impedance spectroscopy:

The electrode resistance as a function of the equilibrium potential was determined by impedance spectroscopy. The electrodes were first equilibrated for one hour at the potential upon the impedance measurement was started at 100 kHz. The bias was set to the equilibrium potential and a sinus potential was applied with an amplitude of 10 mV.

4 Results and Discussion

The hydrogen gas phase absorption/desorption reaction at constant pressure is directly compared with the electrochemical charge discharge process at constant electrochemical potential. The hydrogen absorption and desorption of $LaNi_5$ in the gas phase as a function of the hydrogen gas pressure is shown in figure 2. The equilibrium potential of $LaNi_5$ at room temperature is 2 bar. The hydrogen absorption at a slight overpressure (5 to 10 bar) is completed in less than 100 seconds. The rate of desorption is lower, however, the desorption (0.1 to 0.01 bar) is completed to more than 50% in 60 seconds. The corresponding electrochemical measurement is show in figure 3. The applied potential for the charge process corresponds to a pressure of 2.7 bar. After 31 minutes the charged capacity reaches 50% of the maximum capacity. The same amount of hydrogen is absorbed from the gas phase in 76 seconds. The discharge process is after 13 minutes to 50% completed in the electrochemical measurement while it only takes 53 seconds in the gas phase desorption.

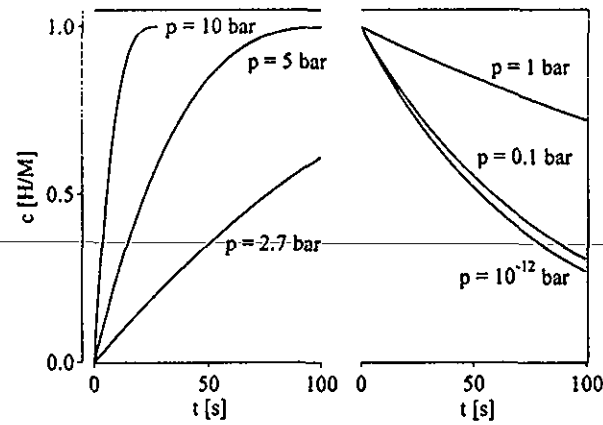

Figure 2: Calculated [16] gas phase absorption (left hand side) and desorption (right hand side) concentrations versus time for $LaNi_5$ at 293 K (isothermal condition). The calculation is based on a model which was experimentally verified. The gas phase hydrogen pressure is indicated in the figure

From this comparison we may conclude that in an electrochemical system the desorption rate is higher than the absorption rate. The applicable potential in the electrochemical measurement is limited to the hydrogen evolution potential (theoretically: -0.926 V vs. the Hg/HgO reference electrode). The hydrogen absorption rate strongly depends on the applied pressure as shown in figure 2. Therefore, the driving force for desorption is higher than for absorption in an electrochemical system. The hydrogen absorption and desorption is much faster in the gas phase (absorption 24 times, desorption 15 times) compared to the electrochemical charge and discharge reaction. Furthermore the low rate of the electrochemical reaction compared with the rate of the gas phase reaction allows to exclude a rate limiting step in the bulk, i.e. absorption in the subsurface layer, diffusion within the host metal, nucleation of the hydride phase, and growth of the hydride phase. These steps are identical for gas phase and electrochemical reaction and therefore not rate determining in the electrochemical reaction. Furthermore, the high absorption rate in the gas phase compared to the electrochemical charge is not an effect of a local temperature increase due

to the heat of formation. If the heat of formation would play an important role in the gas phase kinetics, the desorption should be much slower than the absorption process, and this is not the case.

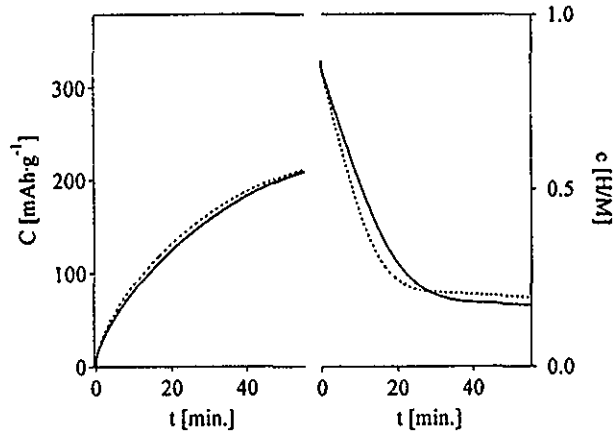

Figure 3: Time resolved absorption and desorption capacity measurement for an AB_5 electrode at T = 291K (solid line) and T = 308 K (dashed line). Hydrogen capacity as a function of time upon a potential step. Absorption measurement from Eeq = -0.787 V to E = -0.940 V(left hand side) followed by the desorption at E = -0.6 Vvs. Hg/HgO (right hand side).

The resistance of an electrode is defined as the ratio of overpotential and applied current. Figure 4 shows the temperature dependence of the resistance. For low temperatures ($280 \leq T \leq 310$ K) the resistance decreases linearly with increasing temperature and remains almost constant for $T > 310$ K. The constant remaining resistance is attributed to the electrode morphology, i.e. grain to grain resistance and contact resistance between grains and current collector. The temperature depending part of the resistance is attributed to the reaction resistance, i.e. electron transfer. Since the electron transfer is an activated process the reaction resistance decreases with temperature and becomes negligible at high temperatures.

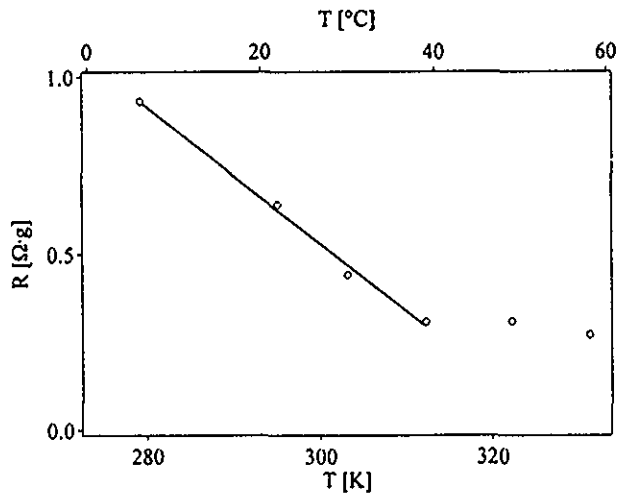

Figure 4: Specific resistance of an AB_5 electrode as a function of the temperature. The resistance was computed from the exchange current density measured by means of the Tafel slope at T = 298K

The resistances of an electrode can be distinguished dependent on the time constant of the process by means of impedance spectroscopy. Five different resistances can be distinguished for the investigated electrode (Fig. 5). The resistance at very high frequencies (R_1, f > 100 kHz) is 0.03 Ω·g and independent of the electrode potential. This resistance is attributed to the electrolyte and depends on the distance between the reference and the working electrode, the type of electrolyte and the concentration of the electrolyte. The second resistance (R_2) is found at a frequency of 4 kHz an is 0.005 Ω·g and increases for more positive potentials. This resistance is attributed to the grain to grain contact. The third resistance (R_3) is attributed to the contact between the metal hydride bed and the current collector and is 0.002 Ω·g. The fourth resistance (R_4) at a frequency of 2 Hz is attributed to the reaction resistance and is 0.07 Ω·g. Finally below a frequency of 50 mHz we find the Warburg impedance (W). The reaction resistance (R_4) strongly depends on the electrode potential as shown in figure 5. The resistance increases over two orders of magnitude in the solid solution phase (α-phase). The main reason for this behavior is the oxidation of nickel and cobalt around -0.82 V vs. the Hg/HgO reference electrode. The grain-grain contact resistance depends on the potential for the same reason. At more positive potentials some species at the surface oxidize and the electrical resistance increases. The increase of the electrode resistance at more positive potential also explains the shape of the discharge curve in figure 3. The discharge current becomes very small when the electrode still contains about one third of the charge.

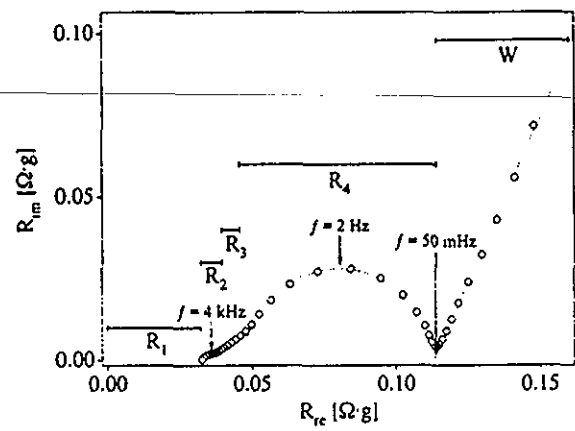

Figure 5: Impedance spectrum of an AB_5 electrode measured in the completely charged state just below the hydrogen evolution at E^0 = -0.016 V (T = 298 K). The first measured point is at R_{re} = 0.04 Ω·g (f = 100 kHz). The spectrum shows a high frequency semi circle with the center at R_{re} = 0.036 Ω·g (f = 4 kHz) and a diameter of 0.007 Ω·g followed by a second semi circle with a center at R_{re} = 0.08 Ω·g (f = 2 Hz) and a diameter of 0.07 Ω·g. Below f ≈ 50 mHz a linear relationship is observed $R_{im} = -11.472 + 2.0251 \cdot R_{re}$ the so called Warburg impedance

5 Conclusion

The simple comparison of gas phase sorption rates with electrochemical sorption rates leads to the conclusion that the rate of the electrochemical sorption is limited by a surface process. The reaction resistance depends as well on temperature (activated process) as on the electrode potential.

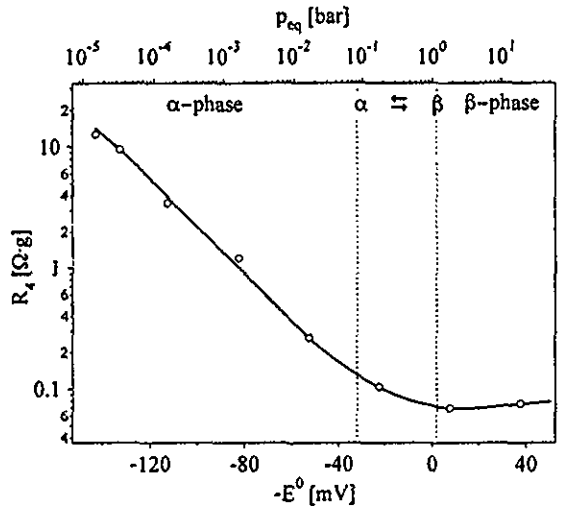

Figure 6: Reaction resistance as a function of the electrode potential (E^0) for the AB_5 alloy sample, (T = 298 K). The resistance was determined from the diameter of the low frequency semi circle

References

[1] J. E. Lennard-Jones, Trans. Faraday Soc. 28 (1932), pp. 333

[2] J. H. Sharp, G. W. Brindley, and B. N. Narahari Achar, Journal of the american ceramic Society 49, No. 7 (1966), pp. 379-382

[3] G. Valensi, Compt. Rend., 202, No. 4 (1936), pp. 309-312

[4] B. V. Erofev, Compt. Rend. Acad. Sci. URSS, 52 (1946), pp. .511-514

[5] P. D. Goodell, G. D. Sandrock and E. L. Huston, J. Less-Common Met. 73 (1980), pp. 135.

[6] P. D. Goodell and P. S. Rudman, J. Less-Common Met. 89 (1983), pp. 117-125.

[7] A. Percheron-Guégan and J.-M. Welter, Chap.2, p. 36 in "Hydrogen in Intermetallic Compounds I", L. Schlapbach (ed.), Springer Series Topics in Applied [16]Y.S. Na, Y. G. Kim, Y. Y. Lee, Int. J. Hydrogen Energy 19 (1994), pp. 899

[8] Ch. N. Park and J. Y. Lee, J. Less-Common Met. 83 (1982), pp. 39-48

[9] T. B. Flanagan, Proc. Int. Symp. on Hydrides for Energy Storage (1977), ed. by A. F. Andresen, A. J. Maeland (Pergamon, Oxford 1978).

[10] N. Kuriyama, T. Sakai, H. Miyamura I. Uehara and H. Ishikawa T. Iwasaki, Journal of Alloys and Compounds 202 (1993), pp. 183-197

[11] A. Züttel, F. Meli and L. Schlapbach, J. of Alloys and Compounds 221 (1995), pp. 207-211.

[12] Y. Fukumoto, M. Miyamoto, M. Matsuoka and C. Iwakura, Electrochimica Acta 40, No. 7 (1995), pp. 845-848.

[13] C. Iwakura M. Miyamoto, H. Inoue, M. Matsuoka, Y. Fukumoto., J. Alloys and Compounds 259 (1997), pp. 129-134.

[14] Y. Sakamoto, K. Kuruma and Y. Naritomi, Ber. Bunsenges. phys. Chem. 96 (1992), pp. 1813.

[15] The temperature dependance of the standard potential of the Hg/HgO reference electrode is $E_{Hg/HgO}$ [V] = $1.18041 - (4.4666 \cdot 10^{-3} - 6.93606 \cdot 10^{-4} \cdot \ln(T)) \cdot T - 1.0788 \cdot 10^{-6} \cdot T^2 + 4.512 \cdot 10^{-10} \cdot T^3 - 5.23 T^{-1}$. J. Balej, Int. J. Hydrogen Energy, Vol. 10, No. 6 (1985), pp. 365-374.

[16] A. Jemni, S. Ben Nasrallah, J. Lamloumi, Int. J. of Hydrogen Energy (1998), in press.

Annex

Relation between pressure and potential

The relation between the equilibrium potential (vs. Hg/HgO reference electrode) of the metal hydride electrode and the equilibrium hydrogen pressure is given by the Gibbs free energy (ΔG):

$$\Delta G = R \cdot T \cdot \ln\left(\frac{p_{eq}}{p_0}\right) = -n \cdot F \cdot \Delta E^0 \tag{1}$$

where R is the molar gas constant ($R = 8.31441\ J \cdot mol^{-1} \cdot K^{-1}$), T is the absolute temperature, p_{eq} is the hydrogen equilibrium pressure of the metal hydride, p_0 is the standard pressure (1.013·105 Pa which corresponds to a $\Delta E^0 = 0$), n is the number of electrons transferred in the reaction (2 electrons in the case of a metal hydride), F is the Faraday constant ($F = 96484.56\ A \cdot s \cdot mol^{-1}$) and ΔE^0 is the equilibrium potential of the metal hydride electrode versus the standard hydrogen electrode ($\Delta E^0 = \Delta E_{MH} - \Delta E_{Hg/HgO}$). The use of a standard hydrogen electrode in an alkaline electrolyte is difficult, therefore a mercury / mercury oxide (Hg/HgO) electrode is usually applied as reference electrode. The Hg/HgO reference electrode exhibits the same dependence on the pH like the hydrogen or the metalhydride electrode. Therefore the measured potentials of the metal hydride electrode referred to Hg/HgO are independent of pH. The standard potential of the Hg/HgO reference electrode at 20°C is $\Delta E_{Hg/HgO} = -926.9$ mV [15].

$$\ln\left(\frac{p_{eq}}{p_0}\right) = -\frac{2 \cdot F}{R \cdot T} \cdot \left(\Delta E_{MH} - \Delta E_{Hg/HgO}\right) \tag{2}$$

A potential change of 29.58 mV corresponds to change over a decade in pressure.